Design, fabrication and performance tests of a HTS superconducting dipole magnet

C. K. Yang, C. S. Hwang, J. C. Jan, F. Y. Lin, and C. H. Chang
M. Fee and M. Christian

Abstract — **The use of HTS (high-temperature superconductor) coils for accelerator magnets decreases significantly the power consumption and operating cost. Therefore, a preliminary study was launched and a prototype of a dipole magnet with HTS coils has been designed and fabricated by NSRRC and HTS-110 Ltd. Although 2G YBCO wire is expected to be used in future HTS applications, it currently requires more joints to form the completed coils. For this reason, we chose 1G BSCCO wires for the HTS coils. Two single-stage pulse-tube refrigerators with one compressor serve to cool the HTS coils of the magnet, but we shall use LN_2 to replace the pulse-tube refrigerators in the future. The HTS magnet is designed to provide a stable field of strength 1.19 T with field homogeneity better than 1.5×10^{-4} in the range of the transverse direction - $20 \le x \le 20$ mm when it operates at 50 K with a current of 110 A. To compare with the field features of copper coil-dipole magnets, a Hall-probe measurement system was used to measure the detailed magnetic field and B-I characteristics of the HTS dipole magnet at NSRRC.**

Index Terms — **High-temperature superconductors, dipole superconducting magnets, BSCCO superconducting wires, magnetic field measurements.**

I. INTRODUCTION

NSRRC (National Synchrotron Radiation Research Center) is constructing a new synchrotron light source, named TPS (Taiwan Photon Source), which has 48 dipole magnets. As these coils are made of copper, the power consumption is huge. As manufacturing techniques have made great progress since 1999, it is now possible to make commercially long multiple-strand wires based on Bi2223 and Bi2212 ceramics in a silver matrix [1], and their current density can exceed 10^4 A cm^{-2} at 77 K in self field. Through this improvement, the number of magnets using Bi2223 in coils is increasing [2,3]. Although the critical current density of 2G YBCO wire is now better than that of 1G BSCCO, BSCCO wires are available in much longer lengths than YBCO wires. Therefore, we selected 1G wire for the production of this HTS dipole magnet. To test the performance of a HTS dipole magnet, we replaced the normal copper coils with Bi2223 HTS coils in a dipole magnet that was originally designed for a TPS lattice magnet. The HTS coils were tested for 72 hours continuously and field measurements were performed to understand the stability and properties of the magnetic field. In addition, according to our estimates of the power consumption between normal copper wire and HTS wire, if 48 HTS-coil dipole magnets in the 3-GeV TPS were operated for 30 years in a closed LN_2 operating mode, the energy consumption could be decreased by a factor of 3.6, relative to copper-coil dipole magnets.

II. ESTIMATES OF ENERGY SAVINGS

Table I shows the thirty-year costs of consumption of input power, magnet cost, maintenance fees, power consumption, and operating costs, in million New Taiwan dollars (MNTD) individually for dipole magnets in three operational modes.

TABLE I INPUT POWER CONSUMPTION AND COST (MNTD) ESTIMATE OVER THIRTY YEARS

	Copper-coil dipole magnets	HTS dipole with LN2 cooling	HTS dipole with individual cryocoolers
Energy consumption /kW	365	100	144
Cooling water/L min^{-1}	750	<50	528
Power cost per year	6.4	1.76	2.5
Cost of the first year	50	125	168
Maintenance fee per year	2	2	10
Total cost of operation 30 years	481	238	543

We can use individual cryocoolers or LN_2 to cool the HTS dipole magnets. The cost manufacture of the cryocooler operation mode magnet is higher than the LN_2 operation mode and is 3 times larger than that for a copper-coil dipole magnet. The maintenance fee of using individual cryocoolers mode is also higher than LN_2 operation mode and the copper-coil. This is why we plan to use LN_2 instead of using the cryocooler mode. However, the energy consumption by using copper-coil is higher than the other two operation modes. Overall, the total cost of HTS coil-dipole magnets with LN_2 cooling mode is half that of using copper-coils as the energy consumption can be decreased by a factor about 3.6.

To maintain reliable operation for the magnetic field test in this work, we used a cryocooler to cool the HTS coils instead of LN_2 because the safe operating temperature of the 1G wire at operating field strength is below 70 K. The cryocooler kept the temperature of the coil below 50 K.

III. DESIGN OF THE DIPOLE MAGNET

A. Design of the magnet yoke

The TPS storage-ring bending dipole is a magnet of type H. Figure 1 shows a cross section of a TPS magnet [4]. This figure shows only the upper half as magnet is symmetrical in the horizontal plane. The yoke was made of low-carbon steel, assembled from 1 mm steel laminations and the copper coils comprised two double-layer, multi-turn copper pancake coils, mounted on the yoke. A 6 mm 45° chamfer at the ends of the pole tips suppressed the sextupole field components. The pole gap is 46 mm pole face width is 172 mm. This magnet provides a bending angle of 7.5° and a bending radius of 8.4033 m along the path of the particle orbit of arc length 1.1 m. The central field is 1.191 T at 615 A for a beam energy of 3 GeV. After using a Hall-probe system to measure the performance of the magnetic field, we removed the copper coils of this magnet and sent it to HTS-110 Ltd (Lower Hutt, New Zealand), where the HTS coils were manufactured to replace the copper coils.
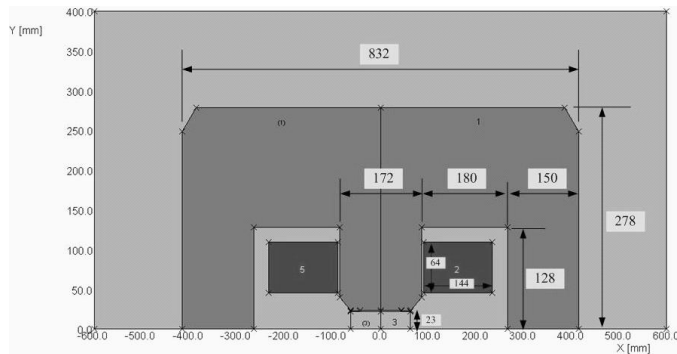

Fig. 1. Cross section of TPS storage ring bending dipole magnet.

B. Design of the HTS coils and force level

To design the HTS coils, we developed both 2D planar and 3D magnetic models with the same yoke dimensions and BH data for the yoke iron. The software package FEMM (Finite-Element Magnetic Modeling) and the magneto-static package Opera [5] were used for the 2D and 3D models. The 2D model was used to ensure that replacement of the low current-density copper coils with high current-density HTS coils would have a negligible effect on the field and its homogeneity, and to determine that ferrous flux-diverters would be useful to protect the HTS coils from excessive perpendicular fields. The 3D model was developed to confirm preliminary results from the 2D analysis, to optimize the dimensions of the flux-deflectors around the entire path of the coil pack, and to calculate the Lorentz and other magnetic forces on the coil pack when the dipole is operated at full field.

According to the simulation results, double pancake with 128 turns per layer were chosen. We chose type HT-SS wire, offered by Sumitomo Electric Industries, because type H has the highest engineering current density within the DI-BSCCO family, and type HT-SS has the best mechanical properties within the type H family [6]. The wire is in the shape of a tape 4.5mm wide and 0.3mm thick and its critical current I_C is larger than 160A (77K, self field, end-to-end).

In our design, the radial outward force on the coil pack is approximately 16 N/cm around the pack, and the maximum value of vertical force is nearly 20N/cm. Due to the weight of the coil pack, a further 1.5N/cm force will add to vertical force on the lower coil but subtract from that on the upper coil.

C. Design of the cryostat and cryocooler connection

The upper and lower coil-packs are each installed in a separate cryostat. Figure 2 shows the exploded view of one the cryostat with a coil-pack enclosed. This cryostat consists of a thick-walled aluminum section with O-ring groves at top and bottom, attached to two 4 mm stainless plates that form the upper and lower faces of the cryostats. At the ends of these cryostats, where they extend out of the yoke, there are flat faces (also O-ring grooved) positioned to connect to the rectangular end-blocks. Openings in these faces allow the copper cold-bus to protrude through for connection to the cold-heads and also allow access for current-leads and sensor wiring.
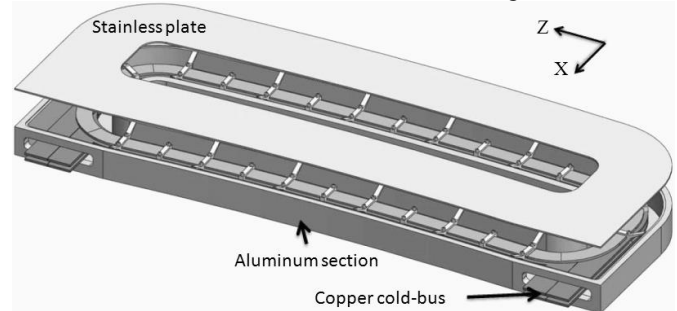

Fig. 2. Exploded view of one of the cryostat with a coil-pack enclosed.

The upper and lower coil-packs are connected to the cryocooler cold heads via flexible high-purity copper straps, to minimize any vibration transfer from the cryocooler cold heads to the coils. These two coil-packs are mounted on rigid G10 supports. In spite of the combined mass of approximately 90 kg, they are only connected to the cryocooler cold heads via flexible straps, so the vibration of the coil-packs is significantly less than 3 μm. Since the magnetic field at the pole is very insensitive to coil-pack movements, the vibration in the coil-pack has a negligible effect on magnetic field quality.

D. Assembly

Cryostat-halves were mounted into the pole-halves, then assembled together. The coils were connected together with superconducting leads and to the current tabs on the end-blocks with resistive current leads. Finally, connections were made between the cold-buses and cryocooler cold heads. Figure 3 shows the photo of the finished retrofitted dipole magnet with original yoke, cryostat, and cold head.
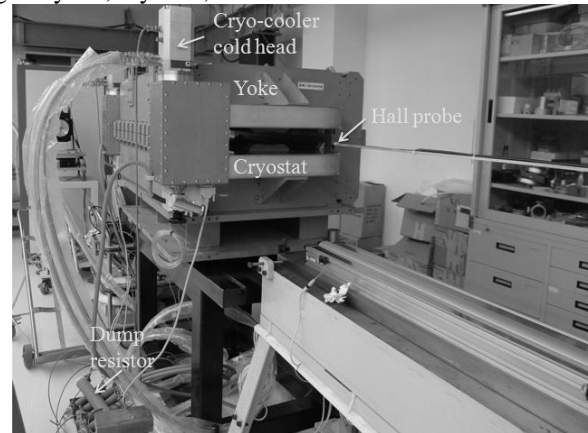

Fig. 3. HTS dipole magnet and the Hall probe measurement system.

E. Quench protection system

This magnet employs three protective systems to detect and avoid possible quench of the superconductor before damage could occur.

Two pairs of voltage taps detect the upper and lower coil voltages (V1 and V2) and the voltage difference between two coils, which are continuously monitored. Ten carbon-ceramic cryogenic thermometers, also continuously monitored, are located among the coils and cold bus to detect thermal variation during operation. The long-term drift of these thermometers is less than 1 mK per year over 20 years and the magnetic field error is less than 1 % in a magnetic field below 6 T.

The interlock state of a magnet monitor system becomes TRUE when the temperature of each sensor decreases through its individually set ENABLE setting. The interlock state switches to FALSE in the event that any voltage or temperature sensor reads above its DISABLE setting. The response time is less that 100 ms, which means the protection system can shut down the power supply before quench can occur. The magnet monitor displays the temperatures and voltages on its front panel and is capable of remote monitoring via RS232 serial-port communications.

The third protective system is an energy-dump circuit with resistors at room temperature, connected in parallel with the HTS coils. The dump resistor is used to absorb the magnetic energy stored in the coils in case of a fault in the power supply. It can prevent an excessive voltage increase in the coils. The magnet has an inductance approximately 1.1 H, but this value is an average as the inductance is greater at small currents because of the behavior of the iron circuit. As the energy stored in the operating magnetic field is approximately 10 kJ, we chose a dump resistor to be approximately 0.7 Ω at maximum power load 3.4 kW, which allows the current to decay with a time constant approximately 1.6 s.

IV. Experimental Setup

We used a helium leak detector (Model ASM 182 TD+, Alcatel Vacuum Technology Corporation) to measure the rate of leakage of the cryostat. Although o-rings seal the vacuum in the cryostat, evident leaks occur at just four locations, and these leakage rates are all less than 7.7×10^{-10} mbar L s^{-1}.

A turbomolecular pumping station (Varian Inc.) took about 24 h to evacuate the cryostat to 2.7×10^{-5} mbar. A cryocooler compressor connected to both cold heads was then activated to cool the HTS coils. The turbopump continued to pump during the cooling of the HTS coils and measurement of the magnetic field. The cryocooler compressor (model CP289c, Cryomech Inc.) has cooling capacity 28 W at 50 K and 40 W at 60 K, and can cool to 30 K with no load. About 20 h was required to cool the HTS coils from room temperature to about 45 K (depending on the thermometer locations). After cooling, the pressure in the cryostat was 3.3×10^{-7} mbar.

A power supply (Agilent Model 6681A) used to charge our HTS coil dipole magnet can provide a current of 500 A and up to 8 V. The magnet monitor connected to the power supply would shut down the power supply if any local temperature, voltage across each coil pack or voltage difference between two coil packs exceeded its safe set point. To ensure that freighting the magnet had caused no problem, we increased the current in a series of conservative steps pausing between steps for several

minutes to confirm that the magnet was stable. At first we stepped the current by 1 A and verified that V1 and V2 were small. We then increased the current in step 10 A up to the operating current, pausing 15 min between steps, and verified V1, V2 and all temperatures of the HTS coils.

We used a Hall probe (Model HHP-MP, Arepoc Ltd., Slovakia) to measure the magnetic field. This probe has ranges $\pm$ 3 T of magnetic field and 1.5 to 350 K of temperature with great sensitivity and linearity. A Teslameter (Model DTM-151 Digital, Group3 Technology Ltd., Auckland New Zealand) was used to read the measurement results of the Hall probe and its resolution for 3.0 T full scale is 0.1G. The Hall probe, fixed on a 1.2-m rod and moved with a three-axis stepping motor, can be seen in Fig. 3. Hall probe mapping trajectories of two kinds were used to measure the magnetic field, and four methods to analyze its behavior [7]. According to the magnet construction, we used the lamination mapping method to measure the magnetic field.

Although the magnetic field nominally operates at 1.191 T, we undertook a soaking test for 72 h and measured the magnetic field at 1.258 T to test the stability and performance of the field of this magnet at a greater operating current. Field deviations $\Delta B/B$ were calculated using the magnetic field at the magnet center; the magnetic field was integrated and expanded with 2-D least-square fitting to calculate the first integrated field deviations $\Delta(\int \ Bds)/\int \ Bds$.

V. Results

A plot of operating current versus central magnetic field during ramp the current up and down is shown in Fig. 4. These data indicate that the deviations of the central magnetic field at the same operating current are less than 1 %. The magnetic fields 1.191 and 1.258 T, at the center of the pole gap, are attained at currents 110.39 and 116.95 A respectively. The influence of iron saturation on the field becomes appreciable above 1.2 T, but that effect is not evident in Fig. 4.
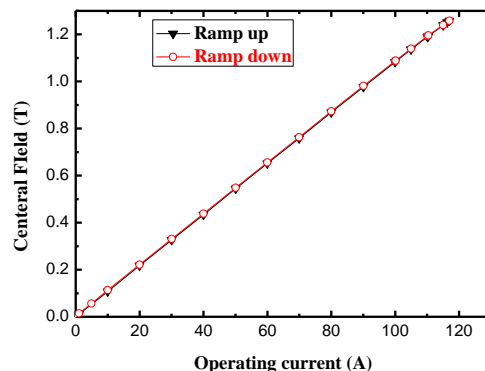

Fig. 4. Operating current vs central magnetic field of the HTS coil magnet.

The result of operation uninterrupted for 72 h at the central magnetic field 1.258 T is shown in Fig. 5. The maximum variation of central field is 0.0007 T, which might come from instability of the power supply. Ten thermometers located along two coils are used to measure the temperature variations of HTS coils during a soaking test for 72 h while the magnet operated at 116.95 A. The temperature fluctuations are less than

0.2 K. The maximum temperature on the coil is below 48 K. The thermal stability is hence satisfactory during operation at high current.

The distributions of the magnetic field along the longitudinal direction of the central axis and ±30 mm from the central axis are presented in Fig. 6. The maximum deviation between these three axes is 0.025 %, which implies that the effective region of homogeneous field extends at least ±30 mm to each side of the central axis.
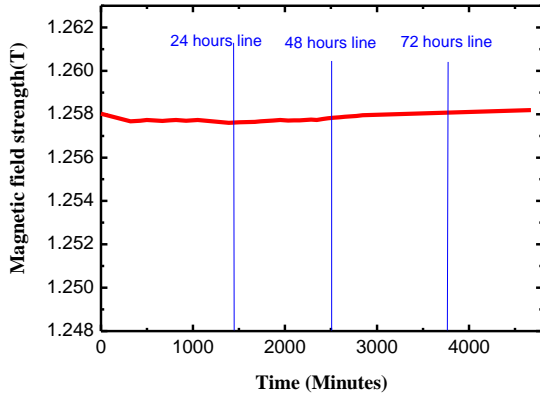

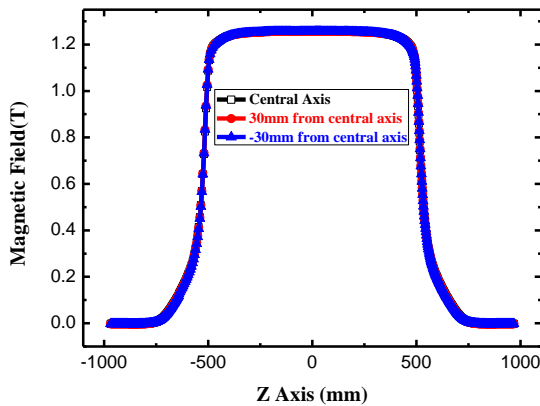Fig. 5. Central magnetic field vs time during a soaking test for 72 h

Fig. 6. Distribution of magnetic field along the longitudinal direction of the central axis and ±30 mm from the central axis.

The field deviations at the center were all within 1.75×10^{-4} (1.66×10^{-4} for the copper dipole magnet) in the range of the transverse direction $-30 \leq x \leq 30$ mm. Integrated field deviations, shown in Fig. 7, are very similar to theoretical results even though there are some differences on x-axis, which also seen in the copper-coil magnet. Furthermore, they are less than $\pm 1.2 \times 10^{-4}$ in the range of transverse direction $-20 \leq x \leq 20$ mm, which is a little better than that of the copper coil-dipole magnet in the same range ($\pm 1.8 \times 10^{-4}$). The asymmetry of the measurements is due to limits in the mechanical precision of manufacture. The small difference between HTS and Copper coil performance comes from the mechanical precision of magnet reassembly and the precision of the Hall probe.
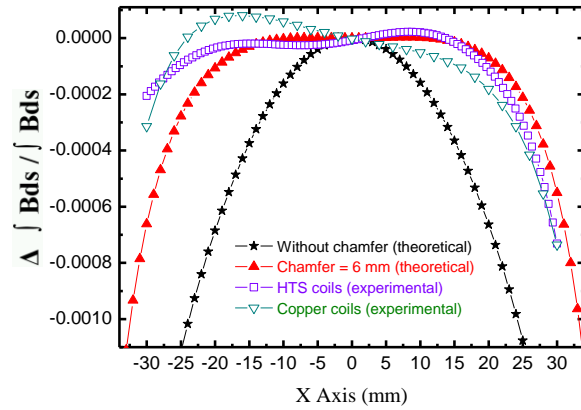

Fig. 7. Integrated field deviations of experimental and theoretical results.

VI. CONCLUSION

A dipole magnet with HTS coils made of 1G BSCCO wires has been designed and fabricated by NSRRC and HTS-110 Ltd. The test results show that the temperature and central magnetic field in continuous operation at current 116.95 A are stable during a 72 h soak test. The field deviations and the integrated field deviations of a HTS coil-dipole magnet and a copper coil-dipole magnet are comparable. These test results show that a concept of replacing copper coils with HTS coils is feasible for a future accelerator.

REFERENCES

[1] L. Mazur, E. Podtburg, D. Buczek, W. Carter, U. Kosasih, S.-J. Loong, K. Manwiller, D. Parker, P. Miles, M. Tanner, J. Scudiere, "Long length manufacturing of BSCCO-2223 wire for motor and cable applications," in *Int. Cryogenic Materials Conf.*, Montreal, Quebece, Canada, 1999.

[2] A. I. Ageev, I. I. Akimov, A. M. Andriishchin, I. V. Bogdanov, S. S. Kozub, K. P. Myznikov, D. N. Rakov, A. V. Rekudanov, P. A. Shcherbakov, P. I. Slabodchikov, A. A. Seletsky, A. K. Shikov, V. V. Sytnik, A. V. Tikhov, L. M. Tkachenko, and V. V. Zubko, "Test results of HTS Dipole," *IEEE Trans. Appl. Supercond.*, vol. 12, pp. 125–128, 2002.

[3] J. Muratore, J. Escallier, G. Ganetis, A. K. Ghosh, R. C. Gupta, P. He, A. Jain, P. Joshi, P. Wanderer, M. Fee, and M. Christian, "Magnetic field measurements of an HTS Retrofit Synchrotron Dipole," *IEEE Trans. Appl. Supercond.*, vol.21, pp. 1653–1656, 2011.

[4] F. Y. Lin, C. S. Hwang, C. Y. Kuo, J. C. Huang, J. C. Jan, H. H. Chen, C.S. Yang, M. H. Huang, C. H. Chuang, "Measurement of accelerator lattice magnet prototypes for TPS storage ring," in *Proc. IPAC'10*, Kyoto, Japan, 2010, p. 319.

[5] A code uses to do electromagnetic design and its description is on http://www.cobham.com/about-cobham/aerospace-and-security/about-us/antenna-systems/kidlington/products/opera-3d.aspx.

[6] N. Ayai, K. Yamazaki, M. Kikuchi, G. Osabe, H. Takaaze, H. Takayama, S. Kobayashi, J. Fujikami, K. Hayashi, K. Sato, K. Osamura, H. Kitaguchi, S. Matsumoto, T. Kiyoshi, and J. Shimoyama, "Electrical and mechanical properties of DI-BSCCO type HT reinforced with metallic sheaths," *IEEE Trans. Appl. Supercond.*, vol. 19, pp. 3014–3017, 2009.

[7] C.S. Hwang, C.H. Chang, P.K. Tseng, T.M. Uen, Joel Le Duff, "Different kinds of analysis methods on a rectangular combined function bending magnet," *Nucl. Instr. and Meth. A* **383** (1996), p. 301.